Cell Reports
Report

Motile Axonal Mitochondria Contribute to the Variability of Presynaptic Strength

Tao Sun,[1,2] Haifa Qiao,[1,2,3] Ping-Yue Pan,[1,4] Yanmin Chen,[1] and Zu-Hang Sheng[1,*]
[1]Synaptic Functions Section, The Porter Neuroscience Research Center, National Institute of Neurological Disorders and Stroke, National Institutes of Health, Room 2B-215, 35 Convent Drive, Bethesda, MD 20892, USA
[2]These authors contributed equally to this work
[3]Present address: Department of Biomedical Sciences, Florida State University College of Medicine, Tallahassee, FL 32306, USA
[4]Present address: Department of Biochemistry, Weill Cornell Medical College, New York, NY 10065, USA
*Correspondence: shengz@ninds.nih.gov
http://dx.doi.org/10.1016/j.celrep.2013.06.040

SUMMARY

One of the most notable characteristics of synaptic transmission is the wide variation in synaptic strength in response to identical stimulation. In hippocampal neurons, approximately one-third of axonal mitochondria are highly motile, and some dynamically pass through presynaptic boutons. This raises a fundamental question: can motile mitochondria contribute to the pulse-to-pulse variability of presynaptic strength? Recently, we identified syntaphilin as an axonal mitochondrial-docking protein. Using hippocampal neurons and slices of *syntaphilin* knockout mice, we demonstrate that the motility of axonal mitochondria correlates with presynaptic variability. Enhancing mitochondrial motility increases the pulse-to-pulse variability, whereas immobilizing mitochondria reduces the variability. By dual-color live imaging at single-bouton levels, we further show that motile mitochondria passing through boutons dynamically influence synaptic vesicle release, mainly by altering ATP homeostasis in axons. Thus, our study provides insight into the fundamental properties of the CNS to ensure the plasticity and reliability of synaptic transmission.

INTRODUCTION

The effects of synaptic variability on neuronal or circuit activity are increasingly recognized. Some degree of variability may be necessary for signal processing in flexible or adaptive systems (Hessler et al., 1993; Murthy et al., 1997; Zador, 1998). A fundamental question is how the variation in synaptic strength arises. In the past decade, numerous studies focused on the structural and stochastic properties of molecular events underlying synaptic variability (see reviews by Atwood and Karunanithi, 2002; Stein et al., 2005; Marder and Goaillard, 2006; Branco and Staras, 2009; Ribrault et al., 2011). These events include opening voltage-dependent Ca^{2+} channels and spacing between the channels and the Ca^{2+} sensor, the fusion modes and kinetics of synaptic vesicles (SVs), content and size of SVs, single versus multiple SV release, and number of receptors at synapses (Liu et al., 1999; Karunanithi et al., 2002; Conti and Lisman, 2003; Edwards, 2007; Young and Neher, 2009). Most of these factors are the basis for marked heterogeneity in synaptic transmission from neuron to neuron or from synapse to synapse. However, it is not known which dynamic process at axonal terminals contributes to pulse-to-pulse variability at single-bouton levels in response to identical synaptic stimulation.

Mitochondria maintain synaptic transmission by producing ATP and buffering Ca^{2+}. Mitochondrial loss from synapses inhibits synaptic transmission due to insufficient ATP supply (Verstreken et al., 2005). Axonal mitochondria undergo dynamic and bidirectional transport, and motile mitochondria can become stationary or pause at synapses and move again in response to physiological changes (see review by Sheng and Cai, 2012). In hippocampal neurons, approximately one-third of axonal mitochondria are motile (Kang et al., 2008). This raises a question: can motile mitochondria influence SV release, thereby contributing to the pulse-to-pulse variability of presynaptic strength? Our recent study identified syntaphilin (SNPH) as a "static anchor" docking mitochondria (Kang et al., 2008). SNPH targets the mitochondrial outer membrane, is sorted to axons via its axon-sorting sequence, and immobilizes axonal mitochondria via its microtubule (MT)-binding domain. SNPH-MT interaction is stabilized by dynein light-chain LC8 (Chen et al., 2009). Deleting murine *snph* recruits the majority of axonal mitochondria into motile pools, whereas overexpressing SNPH abolishes their motility. Thus, *snph* mice provide us with a unique genetic tool to address whether changes in axonal mitochondrial motility compromise the variability of presynaptic strength.

RESULTS AND DISCUSSION

Mitochondrial Motility Correlates with the Pulse-to-Pulse Variation of EPSC Amplitudes

By using cultured hippocampal neurons from $snph^{+/+}$ and $snph^{-/-}$ mouse littermates, we first examined whether axonal

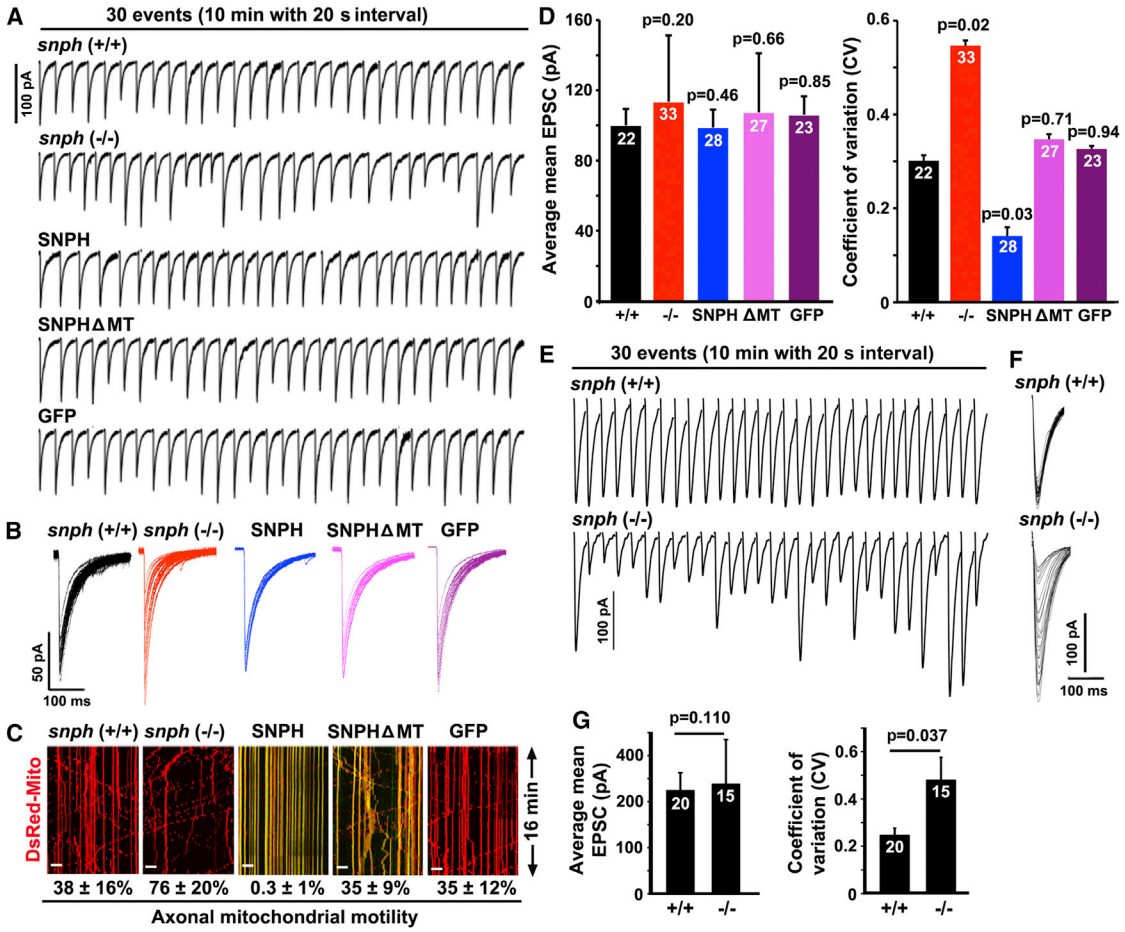

Figure 1. Axonal Mitochondrial Motility Correlates with the Pulse-to-Pulse Variation of EPSC Amplitudes

(A–C) Single trace (A) and superimposed traces of 30 sweeps (B) at 0.05 Hz stimulation and kymographs of axonal mitochondrial motility (C) from hippocampal neurons of *snph*$^{+/+}$ or *snph*$^{-/-}$ mouse littermates, or WT neuron pairs, where presynaptic neurons expressing EGFP-SNPH, EGFP-SNPHΔMT, or GFP form synapses with untransfected postsynaptic neurons. Mitochondria were labeled with dsRed-mito (red). Neurons were transfected at 7–8 DIV; EPSCs were recorded 3 days after transfection. In kymographs, vertical lines represent stationary organelles; oblique lines or curves to the right indicate anterograde transport. Scale bars represent 10 μm (C).

(D) Axonal mitochondrial motility influences the pulse-to-pulse synaptic variability. A total of 30 traces from each neuron pair were averaged, and data in the same group were pooled to calculate the average mean peak EPSC amplitude (left). The CV of pulse-to-pulse EPSC amplitudes was analyzed from 30 sweeps (right).

(E–G) Increasing mitochondrial motility enhanced synaptic fluctuations in acute hippocampal slices. Sample traces of the middle 30 EPSC events from 90 to 120 (E) and superimposed 200 EPSC events (F) and mean peak EPSC amplitude and relative CV values (G) from *snph*$^{+/+}$ or *snph*$^{-/-}$ littermates (postnatal 3–5 weeks) are shown. Each recording was evoked by 0.05 Hz stimulation via the Schaffer collateral pathway. A total of 200 sweeps from each slice were averaged, and the data in the same group were pooled to calculate the mean peak EPSC amplitude.

Data were collected from the total number of neurons (D) or slices (G) indicated within bars. Data sets (D) were analyzed by the nonparametric Kruskal-Wallis test ($p = 0.029$, right panel) comparing the five groups. The Dwass-Steel-Critchlow-Fligner post hoc analysis was applied for multigroup comparison. The p values on top of bars in (D) are pairwise comparisons to *snph*$^{+/+}$ neurons. Data sets were also $\log_{10}$ transformed to normalize distribution, followed by one-way ANOVA analysis and the Dunnett test for multigroup CV comparison of (D) ($p = 0.027$, right panel). Data sets in (G) were analyzed using the nonparametric Mann-Whitney U test for two groups. Error bars, SEM.

See also Figure S1 and Movies S1, S2, S3, and S4.

mitochondrial motility influences mean amplitudes of excitatory postsynaptic currents (EPSCs) and their pulse-to-pulse variation. Representative and superimposed traces of 30 sweeps (Figures 1A and 1B) in *snph*$^{-/-}$ neurons showed a larger fluctuation in EPSC amplitude under 0.05 Hz stimulation compared with *snph*$^{+/+}$ neurons. Elevated expression of EGFP-SNPH, but not EGFP-SNPHΔMT, a docking loss-of-function mutant, further reduced the variation found in wild-type (WT) neurons. Deleting *snph* robustly increased axonal mitochondrial motility (76% ± 20%, n = 17; $p < 0.01$) (Figure 1C) relative to WT neurons (38% ± 16%, n = 15). Conversely, overexpressing SNPH abolished axonal mitochondria motility (0.3% ± 1%, n = 19; $p < 0.01$). Although axonal mitochondrial motility did not impact the mean EPSC amplitudes, it significantly influenced the variability of pulse-to-pulse EPSC amplitudes (Figure 1D). The coefficient of variation (CV) of EPSC amplitudes was larger in *snph*$^{-/-}$

neurons (CV, 0.546 ± 0.011; p = 0.017) compared to *snph*$^{+/+}$ neurons (CV, 0.301 ± 0.012). In contrast, elevated SNPH expression further reduced the CV (0.141 ± 0.017; p = 0.028) found in WT neurons. As controls, expressing SNPHΔMT or GFP had no effect on mitochondrial motility (35% ± 9% and 35% ± 12%, respectively; p > 0.05) and on CV values (0.347 ± 0.011 and 0.326 ± 0.006, p = 0.713 and p = 0.941, respectively) relative to WT neurons. Pearson correlation analysis revealed a significant positive correlation (r = 0.988; p = 0.002) between the motility of axonal mitochondria and the CV values of pulse-to-pulse EPSC amplitudes.

We next examined synaptic fluctuation in acute hippocampal slices from *snph*$^{+/+}$ and *snph*$^{-/-}$ mouse littermates by recording 200 EPSC events evoked by 0.05 Hz stimulation in Schaffer collateral synapses. Enhancing axonal mitochondrial motility by deleting *snph* robustly increased EPSC fluctuation (Figures 1E and 1F). The pulse-to-pulse variability (Figure 1G) was significantly increased in *snph*$^{-/-}$ mice (CV, 0.479 ± 0.098; p = 0.037) relative to WT littermates (CV, 0.246 ± 0.031). Due to its specific targeting to axonal but not dendritic mitochondria (Kang et al., 2008), SNPH influences pulse-to-pulse EPSC variability likely through a presynaptic mechanism. This was confirmed in cultured neuron pairs where only presynaptic neurons expressing SNPH were selected for recording (Figures 1A and 1B). The kinetics of EPSCs does not show statistical differences in the half-width, rise and decay times, and slopes of EPSCs between *snph*$^{+/+}$ and *snph*$^{-/-}$ hippocampal slices (see Extended Results), indicating that the variation is unlikely from asynchronous SV release. Thus, our results support that axonal mitochondrial motility impacts pulse-to-pulse variability of presynaptic strength.

Given the facts that (1) EPSCs were averaged through summation of the currents from multiple synapses between neuron pairs and (2) mitochondria dynamically pass by or pause at synapses, we assume that mitochondrial motility patterns on individual boutons are highly variable. To test this hypothesis, we further identified five motility patterns of axonal mitochondria at boutons during a 16 min recording time: stationary mitochondria sitting out of synapses (54.07% ± 2.53%) or within synapses (16.29% ± 1.66%); moving mitochondria passing through synapses (14.77% ± 1.58%); or pausing at synapses for a short (<200 s, 7.01% ± 1.29%) or a longer time period (>200 s, 8.30% ± 1.52%) (Figure S1; Movie S1). Our findings are consistent with a previous study in cortical neurons by Chang et al. (2006). Thus, variable patterns of mitochondrial motility at individual boutons are likely one of the main sources contributing to the variability of EPSC amplitudes, which was further supported by genetic manipulation: either immobilizing axonal mitochondria by overexpressing SNPH or increasing their motility by deleting *snph* in neurons (Figures 1A–1D).

Mitochondrial Motility Influences SV Release at Single-Bouton Levels

Our previous study showed that increased mitochondrial motility in *snph*$^{-/-}$ neurons has no impact on quantal size (Kang et al., 2008). To examine presynaptic variability at single-bouton levels, we examined two dynamic events by dual-color live imaging of axonal mitochondria labeled with dsRed-mito and SV release using synapto-pHluorin (spH). All dsRed-mito signals along axons were colabeled by cytochrome *c* (see Extended Results). spH is a SV-targeted and pH-sensitive GFP whose fluorescence is quenched by intraluminal acidic pH but increases upon exocytosis when it is exposed to the neutral pH of the extracellular medium. Thus, changes in spH fluorescence reflect the relative strength of SV release and recycling (Sankaranarayanan and Ryan, 2000). Because of technical limitation in resolving single action potential (AP)-induced spH responses, we instead used trains of stimulation (20 Hz, 10 s) to provide a sufficient signal-to-noise ratio (Sun et al., 2010). We reasoned that if variability arises from moving mitochondria, single-bouton responses to each train of stimulation should display different spH ΔF_{peak} values in correlation with mitochondrial distribution and motility.

We first determined whether mitochondrial motility impacts SV release during four successive train stimulations with 100 s intervals by examining three patterns of mitochondrial distribution and motility: (1) boutons with and without a stationary mitochondrion (Figure 2A), (2) boutons with a mitochondrion moving out (Figure 2B), and (3) boutons with a mitochondrion passing by (Figure 2C) during four trains of stimulation. SV release in response to the first train was unaffected by the presence or absence of a presynaptic mitochondrion. SV release remained stable at boutons with a stationary mitochondrion (Figures 2A–2C), whereas SV release was depleted starting at the second train at boutons lacking a mitochondrion (Figure 2A). Interestingly, motile mitochondria significantly impact SV release, which was quickly reduced when a mitochondrion moved out of the boutons (Figure 2B). Conversely, a mitochondrion passing by boutons enhanced SV release (Figure 2C). Analysis of relative ΔF_{peak} values revealed a larger variation in SV release during repeated stimuli at boutons when a mitochondrion is moving out or passing by (Figures 2E and S2C). Consistently, mitochondrial motility also influenced SV release in response to a shorter stimulation train (10 Hz, 5 s with 100 s interval) (Figures S2A and S2B).

We analyzed CV values of ΔF_{peak} variation at each bouton during repeated trains and then averaged CVs over all the trains from each group of boutons (Figures 2E and S2C). In boutons with a motile mitochondrion, the average CV value (0.154 ± 0.021) was substantially higher relative to those from boutons with a stationary mitochondrion (0.061 ± 0.009; p < 0.001) or lacking a mitochondrion (0.081 ± 0.010; p < 0.001). Thus, motile mitochondria, when passing by terminals, contribute to larger variations in SV release. We further studied the variability in single-bouton levels with different total axonal mitochondria motility: (1) WT neurons, 38% ± 16%; (2) neurons with elevated SNPH expression, 0.3% ± 1%; (3) *snph*$^{-/-}$ neurons, 76% ± 20%; and (4) neurons expressing Miro1, 79% ± 3%. Miro1 is a mitochondrial adaptor for linking kinesin motors (Figure 2F; Movies S2, S3, and S4). Enhanced motility of axonal mitochondria in *snph*$^{-/-}$ neurons and in neurons expressing Miro1 led to higher CV values of ΔF_{peak} during stimulation trains: *snph*$^{-/-}$ (CV, 0.30 ± 0.04; p = 0.010) and Miro1 (CV, 0.33 ± 0.03; p = 0.007) relative to WT neurons (CV, 0.18 ± 0.03) (Figure 2G). In contrast, CV was reduced in neurons overexpressing SNPH (CV, 0.11 ± 0.04; p = 0.035). Pearson correlation analysis revealed significant positive correlation (r = 0.987; p = 0.015)

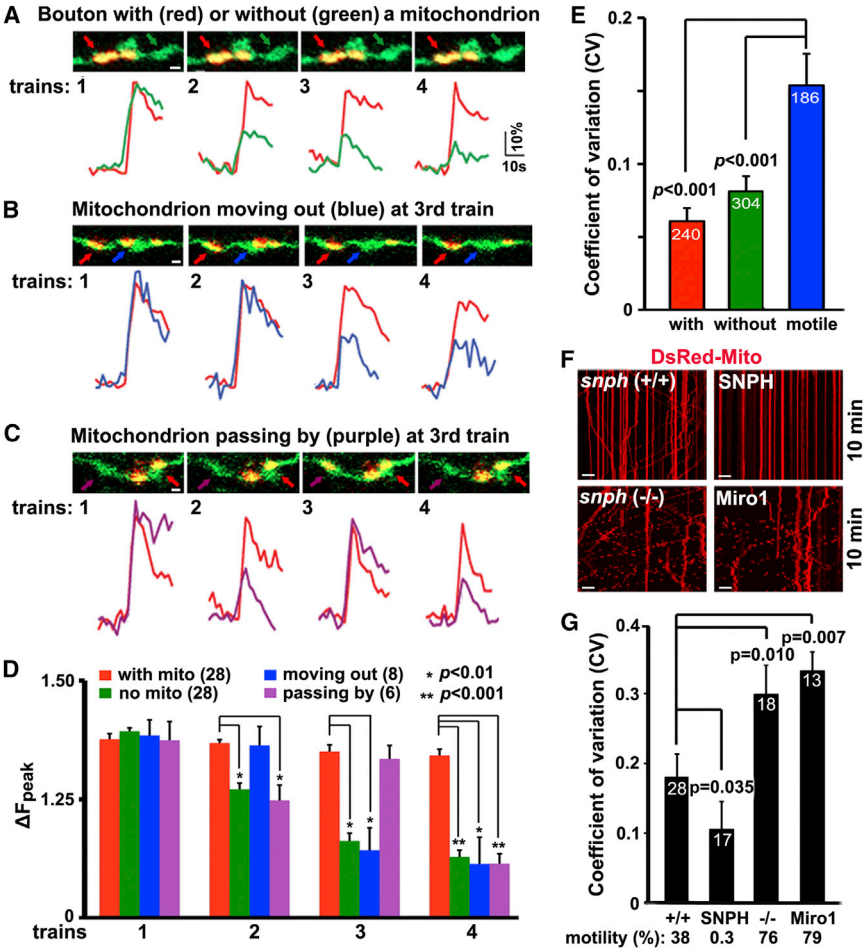

Figure 2. Mitochondrial Motility Influences SV Release at Single-Bouton Levels

(A–D) Dual-color live imaging shows the distribution and motility of axonal mitochondria at boutons and corresponding spH traces (A–C) and normalized spH ΔF_{peak} (D) during four trains of stimulation (20 Hz at 10 s with 100 s interval). Note that SV exocytosis remained robust and stable at boutons with a stationary mitochondrion (red arrows/traces), whereas exocytosis diminished starting at the second train at mitochondrion-free boutons (green arrows/traces) or when a mitochondrion is moving out of the bouton at the third train (blue arrows/traces). A mitochondrion passing by bouton during the third train rescued SV release (purple arrows/traces).

(E–G) Mitochondrial motility influences ΔF_{peak} variability. CV values of the ΔF_{peak} variation at each bouton during repeated stimulation were quantified and then averaged over all the trains from each group of boutons (E) with (red) or without (green) a stationary mitochondrion, or with a motile mitochondrion (blue). Representative spH traces are shown in Figure S2C. Kymographs (F) and average CV values (G) reflect the trial-to-trial ΔF_{peak} variation at each bouton in *snph*$^{+/+}$, *snph*$^{-/-}$, or in neurons overexpressing SNPH or Miro1 (Kruskal-Wallis test for comparing all four groups, $p < 0.0001$) (also see Movie S2, S3, and S4).

Data were collected from the number of neurons indicated in parentheses (D) or from the number of boutons (E) or neurons (G) indicated within bars and analyzed by the nonparametric Kruskal-Wallis test for comparing multiple groups, followed by the Dwass-Steel-Critchlow-Fligner post hoc analysis for all pairwise comparisons. The Mann-Whitney U test was applied for pairwise comparisons for two groups. Error bars, SEM. Scale bars, 1 μm (A–C) and 10 μm (F).

See also Figure S2 and Movies S2, S3, and S4.

between the motility of axonal mitochondria and the average CV values of ΔF_{peak}.

Because the spH response reflects the balance of exo- and endocytosis, we applied 2 μM bafilomycin A1 (Baf), a reacidification blocker, after the third train to trap SVs in the neutral pH environment; hence, ΔF_{peak} at the fourth train mainly reflects exocytosis. Compared to boutons with a stationary mitochondrion in the presence of Baf, ΔF_{peak} remained smaller at boutons lacking a mitochondrion, suggesting that the reduced spH response was mainly due to altered SV exocytosis (Figures 3A and 3B). We further compared the size of releasable SV pools at terminals with versus without a mitochondrion in the presence of Baf by eliciting four trains of stimulation. ΔF_{peak} values for the first train were similar at both types of boutons. However, the difference was observed at the second train and became larger at the third and fourth trains (Figures 3C and 3D), indicating a smaller size of total releasable SVs in terminals without a mitochondrion. Our results are consistent with a previous study showing that depleting mitochondria within axonal terminals results in a faster SV depletion following intensive stimulation (Verstreken, et al., 2005).

ATP Homeostasis Is Critical to Maintain SV Release

Mitochondria maintain presynaptic homeostasis by supplying ATP and by buffering Ca^{2+} during intense, prolonged stimulation (Tang and Zucker 1997; Verstreken et al., 2005; Kang et al., 2008). ATP supports synaptic functions including SV mobilization and fusion and generation of synaptic membrane potentials. To examine the role of axonal mitochondria in maintaining ATP homeostasis during repeated trains of stimulation, we applied an engineered fluorescent ATP sensor Perceval (Berg et al., 2009). The fluorescence intensity ratio (F_{488nm}/F_{405nm}) of Perceval reflects the relative ATP/ADP ratio, thus allowing temporal and spatial detection of physiological changes in cellular ATP levels in live neurons. At resting condition, the axonal ATP/ADP ratio was similar with versus without a mitochondrion. However, when neurons were stimulated with repeated trains (20 Hz for 10 s with 100 s intervals), the ATP/ADP ratio drops significantly, reflecting ATP consumption during neuronal firing and SV release. Within axonal terminal areas (2 × 2 μm) containing a stationary mitochondrion, the ATP/ADP ratio was recovered just before the next train of stimulation (Figure 4A). In contrast, within mitochondrion-free areas, the ATP/ADP ratio

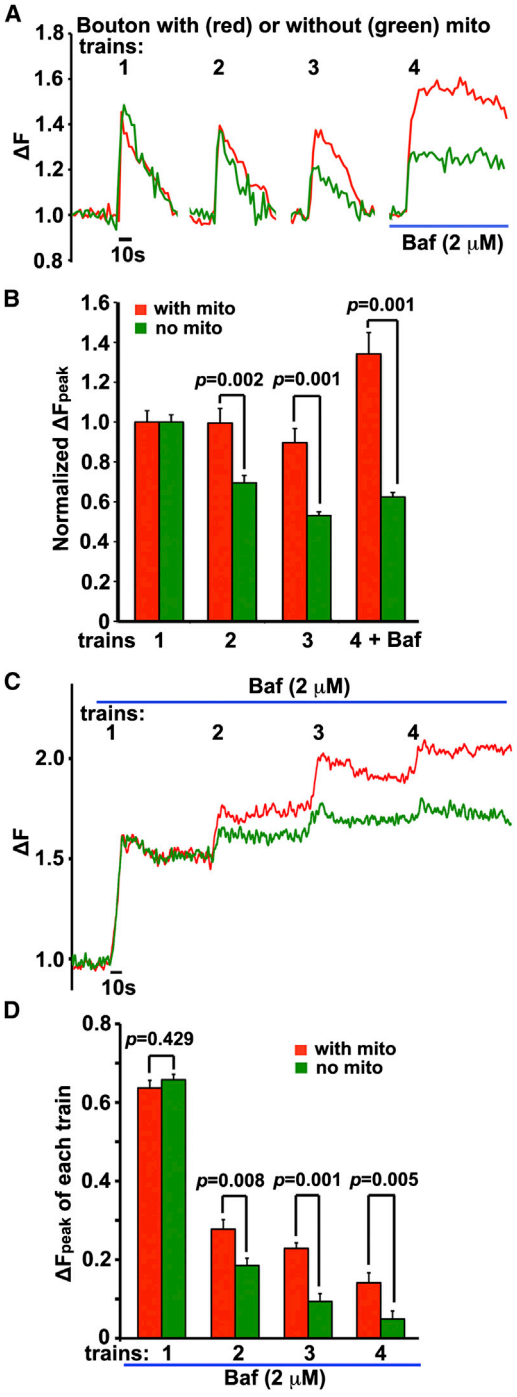

Figure 3. Impact of Presynaptic Mitochondria on the Size of Releasable SV Pools

(A and B) Representative spH traces (A) and normalized ΔF_{peak} (B) before and after applying Baf (2 μM) at the fourth train of stimulation.

(C and D) Representative spH traces (C) and step increase of ΔF_{peak} in response to each train (D) when applying Baf (2 μM) during repeated stimulation.

Data were collected from three neurons (10–50 boutons from each neuron) and analyzed by the Dwass-Steel-Critchlow-Fligner post hoc analysis for all pairwise comparisons. The Mann-Whitney U test was applied for pairwise comparisons for two groups. Error bars, SEM.

before the second train was slightly lower ($p = 0.059$) but was substantially lower ($p < 0.007$) before the third train, reflecting reduced ATP supply after each train of stimulation. Because intracellular pH values impact the Perceval fluorescent intensity (Berg et al., 2009), we monitored pH in the axonal terminals using the pH dye SNARF-5F. Axonal pH values undergo very minor changes (7.1–7.3) during the stimulation regardless of whether with or without a mitochondrion (Figure 4B). Thus, dynamic changes in the ATP/ADP ratios during trains of stimulation are physiologically relevant to the strength of SV release (Figures 2A and 2D). ATP production by presynaptic mitochondria is critical for maintaining SV release. Our results are also consistent with a recent biochemical study in hippocampal synaptosomes, where inhibition of mitochondrial oxidative phosphorylation resulted in a substantial drop in ATP levels accompanied by reduced evoked SV release and unchanged cytosolic calcium levels (Ivannikov et al., 2013). Thus, axonal mitochondrial distribution and motility contribute to the variability of SV release likely by influencing presynaptic ATP homeostasis.

To determine whether the ATP production by mitochondria is critical to maintain SV release, we treated neurons for 15 min with 4 μg/ml oligomycin, an inhibitor of mitochondrial ATP generation. The spH response to the first train was not affected by oligomycin (Figure 4C). In boutons with a mitochondrion, there is no significant change ($p = 0.67$) in the average ΔF_{peak} upon the first train between control (1.37 ± 0.04) and oligomycin-treated groups (1.39 ± 0.10). Consistently, in boutons without a mitochondrion, no ΔF_{peak} change ($p = 0.95$) was observed between control (1.39 ± 0.01) and oligomycin-treated groups (1.38 ± 0.07). Given the fact that oligomycin only blocks new ATP production, after pre-existing ATP was largely depleted beginning at the third train (Figure 4A), ΔF_{peak} was reduced at boutons when mitochondrial ATP production was blocked (Figure 4C), a phenotype mimicking boutons lacking mitochondria. These results highlight a critical role of mitochondria in maintaining synaptic transmission by supplying ATP.

Altered spH response in single-bouton levels may represent a different phenomenon from the observed EPSC variability recorded from multiple synapses between paired neurons. Approximately 30% of mitochondria dynamically move along axons (Figure S1; Movies S1 and S2); EPSC variability during low-stimulation frequency (Figure 1) is likely contributed by summation of many small changes in ATP levels at each synapse during a short timescale. Due to the insufficient spH signal-to-noise ratio in response to the single AP, we are unable to estimate release probability with the imaging approach.

Synaptic mitochondria efficiently buffer presynaptic $[Ca^{2+}]_i$ during intensive synaptic activity (Tang and Zucker, 1997). To determine whether mitochondria have any impact on the basal and evoked $[Ca^{2+}]_i$ under our stimulation profile, we applied two calcium indicators. First, we applied the YFP/CFP ratiometric calcium indicator YC3.60 to monitor the basal and evoked $[Ca^{2+}]_i$ transients during the four trains of stimulation (20 Hz, 10 s with 100 s interval). The YFP/CFP ratio curves reflect the relative $[Ca^{2+}]_i$ levels (Figures S3A and S3B). The basal $[Ca^{2+}]_i$ is defined by averaging YFP/CFP ratios during a 10 s period just before each train (Figure S3C), whereas the evoked $[Ca^{2+}]_i$ is reflected by the total YFP/CFP value during each train of stimulation

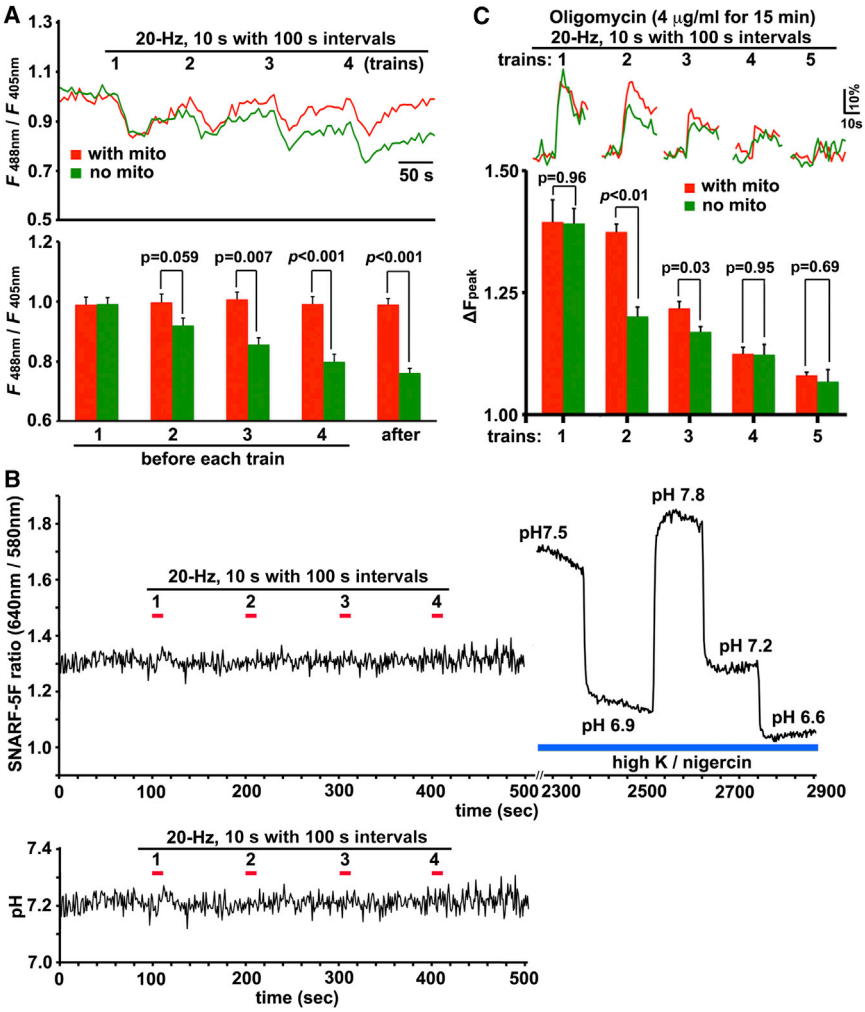

Figure 4. ATP Homeostasis Is Critical to Maintain SV Release

(A) The cellular ATP/ADP ratio during trains of stimulation. The curve of fluorescence intensity (F_{488nm}/F_{405nm}) (upper panel) reflects the relative ATP/ADP ratio. The normalized F_{488nm}/F_{405nm} ratio (lower panel) was recorded before each train.

(B) Measurement of axonal pH using SNARF-5F during trains of stimulation. A total of 20–50 areas with or without a mitochondrion along each axon were selected for imaging. SNARF-5F was excited at 488 nm and detected around 580 and 640 nm during four trains of stimulation, as indicated by red bars (upper left). At the end of stimulation, SNARF-5F signal was calibrated using various buffered solutions containing high K/nigericin with varying pH values (blue bar, upper panel). Calibrated pH values (lower panel) were averaged from 50 axonal terminal areas.

(C) Representative spH traces (upper) and normalized spH ΔF_{peak} (lower) show reduced SV release at boutons with a stationary mitochondrion under treatment with 4 μg/ml oligomycin for 15 min. Note that oligomycin reduced exocytosis at the third stimulus at boutons with a mitochondrion (red), a phenotype similar to the bouton without a mitochondrion (green).

Data were collected from 11 neurons (A) or 5 neurons (C). A total of 10–50 boutons or axonal areas were imaged for each neuron. Data sets were analyzed by the nonparametric Kruskal-Wallis test for comparing multiple groups. The Mann-Whitney U test was applied for pairwise comparisons for two groups. Error bars, SEM.

See also Figures S3 and S4.

(Figure S3D). The YC3.60 ratio-metric imaging shows no significant change in the basal ($p = 0.413$) and evoked $[Ca^{2+}]_i$ ($p = 0.476$) with or without a mitochondrion. Alternatively, we confirmed the evoked $[Ca^{2+}]_i$ transient by using the single-color genetic variant of GCaMP3 calcium indicator GECO (*g*enetically encoded *c*alcium indicator for *o*ptical imaging). The change in GECO fluorescence intensity over baseline ($\Delta F/F_0$) showed fast rising upon stimulation (Figures S3E and S3F). Normalized peak values of $\Delta F/F_0$ over baseline ($p = 0.07$; Figure S3G) and the total increase in normalized GECO intensity during each train of stimulation ($p = 0.08$; Figure S3H) show no significant difference with or without a mitochondrion. Altogether, our studies consistently show that axonal mitochondria have no detectable impact on the basal and evoked $[Ca^{2+}]_i$ under our simulation profile.

We next asked whether increased Ca^{2+} influx or altered Ca^{2+} buffering contributes to the variability of spH responses. Under 10 mM $[Ca^{2+}]_{ex}$, the first ΔF_{peak} value (1.71 ± 0.02; $p < 0.001$) (Figure S4A) is significantly larger than that under 2 mM $[Ca^{2+}]_{ex}$ (1.40 ± 0.03) (Figure 2). However, mitochondria are still required to maintain SV release during four trains of stimulation (Figure S4A). Conversely, incubation with 100 μM EGTA-AM for 3 min has no detectable impact on SV release at boutons with a stationary mitochondrion or on reduced SV release at boutons without a mitochondrion (Figures S4B and S4C), although the first ΔF_{peak} value under EGTA-AM (1.25 ± 0.02; $p < 0.001$) is significantly smaller than that under 2 mM $[Ca^{2+}]_{ex}$ (1.40 ± 0.03) (Figure 2). Therefore, altered levels of ATP, but not $[Ca^{2+}]_i$, are likely one of the major sources contributing to the presynaptic variability in response to identical stimulation.

In the current study, we simultaneously imaged both axonal mitochondria and SV release from single boutons during trains of stimulation. These procedures allowed us to measure the variation of SV release under different patterns of mitochondrial distribution and motility (see Extended Discussion). It is conceivable that the absence of a stationary mitochondrion within an axonal terminal reduces local ATP supply and that a motile mitochondrion passing through a bouton temporally and spatially influences ATP homeostasis, thus impairing ATP-dependent processes at synaptic terminals including SV pool replenishment (Heidelberger et al., 2002). Although presynaptic mitochondria are crucial to maintain the proper size of total releasable SV pools during trains of stimulation, it is possible that other ATP-dependent processes may collectively contribute to presynaptic

variability when mitochondria travel along axons and move into or pass by boutons. Thus, our study revealed that the dynamic movement of axonal mitochondria is one of the primary mechanisms underlying the pulse-to-pulse variability or the trial-to-trial variation of presynaptic strength in the CNS.

EXPERIMENTAL PROCEDURES

Dual patch-clamp EPSC recordings in cultured hippocampal neurons were made with a whole-cell configuration. After identifying paired neurons, APs were detected under current clamp by injecting 400 pA of current (depolarization); only those neurons with resting membrane potentials around −60 mV were selected for paired recording. The hippocampal slice in the recording chamber was superfused with ACSF (1 ml/min) supplemented with picrotoxin (50 μM) and saturated with 95% O_2/5% CO_2. After obtaining stable currents, 200 sweeps were recorded at a holding potential of −70 mV. A total of 50 μM picrotoxin and 100 μM cyclothiazide was applied in the bath solution to block GABA receptor currents and avoid desensitization of postsynaptic receptors during recording.

Dual-color time-lapse imaging was performed to monitor mitochondrial movement and SV release at presynaptic boutons. Neurons at 7–9 DIV were cotransfected with spH and dsRed-mito using calcium phosphate method, followed by imaging at 12–14 DIV. A total of 10–50 boutons were imaged for each neuron examined. The engineered fluorescent sensor Perceval was used to monitor the ATP/ADP ratio in live neurons. Perceval was cotransfected with dsRed-mito and SNPH into neurons at 7–9 DIV. Axonal areas (2 × 2 μm) containing or lacking a mitochondrion were selected for imaging. Perceval was excited at 405 and 488 nm and detected in the 505–550 nm range. The fluorescence intensities (F_{488nm}/F_{405nm}) reflect the relative cellular ATP/ADP ratio. Intracellular pH values were also monitored with the pH indicator dye SNARF-5F.

Animal care and use were carried out in accordance with NIH guidelines and approved by the NIH, NINDS/NIDCD Animal Care and Use Committee. See the Extended Experimental Procedures for additional materials and methods.

SUPPLEMENTAL INFORMATION

Supplemental Information includes Extended Results, Extended Discussion, Extended Experimental Procedures, four figures, and four movies and can be found with this article online at http://dx.doi.org/10.1016/j.celrep.2013.06.040.

ACKNOWLEDGMENTS

We thank J. Diamond, W. Lu, C.J. McBain, and L.-G. Wu for helpful discussions, G. Yellen for the ATP sensor Perceval, J. di Giovanni and B. Zhou for statistical analysis, the members of the Z.-H.S. lab for technical assistance and discussion, and D. Schoenberg for editing. The work was supported by the Intramural Research Program of NINDS, NIH (to Z.-H.S.). T.S. conducted all imaging analysis. H.Q. conducted electrophysiological analysis. P.-Y.P. did preliminary study on the mouse model. Y.C. analyzed mitochondrial motility. Z.-H.S. is a senior author who designed the project, coordinated experiments, and wrote the manuscript.

Received: November 25, 2012
Revised: April 29, 2013
Accepted: June 28, 2013
Published: July 25, 2013

REFERENCES

Atwood, H.L., and Karunanithi, S. (2002). Diversification of synaptic strength: presynaptic elements. Nat. Rev. Neurosci. *3*, 497–516.

Berg, J., Hung, Y.P., and Yellen, G. (2009). A genetically encoded fluorescent reporter of ATP:ADP ratio. Nat. Methods *6*, 161–166.

Branco, T., and Staras, K. (2009). The probability of neurotransmitter release: variability and feedback control at single synapses. Nat. Rev. Neurosci. *10*, 373–383.

Chang, D.T., Honick, A.S., and Reynolds, I.J. (2006). Mitochondrial trafficking to synapses in cultured primary cortical neurons. J. Neurosci. *26*, 7035–7045.

Chen, Y.M., Gerwin, C., and Sheng, Z.H. (2009). Dynein light chain LC8 regulates syntaphilin-mediated mitochondrial docking in axons. J. Neurosci. *29*, 9429–9438.

Conti, R., and Lisman, J. (2003). The high variance of AMPA receptor- and NMDA receptor-mediated responses at single hippocampal synapses: evidence for multiquantal release. Proc. Natl. Acad. Sci. USA *100*, 4885–4890.

Edwards, R.H. (2007). The neurotransmitter cycle and quantal size. Neuron *55*, 835–858.

Heidelberger, R., Sterling, P., and Matthews, G. (2002). Roles of ATP in depletion and replenishment of the releasable pool of synaptic vesicles. J. Neurophysiol. *88*, 98–106.

Hessler, N.A., Shirke, A.M., and Malinow, R. (1993). The probability of transmitter release at a mammalian central synapse. Nature *366*, 569–572.

Ivannikov, M.V., Sugimori, M., and Llinás, R.R. (2013). Synaptic vesicle exocytosis in hippocampal synaptosomes correlates directly with total mitochondrial volume. J. Mol. Neurosci. *49*, 223–230.

Kang, J.S., Tian, J.H., Pan, P.Y., Zald, P., Li, C., Deng, C., and Sheng, Z.H. (2008). Docking of axonal mitochondria by syntaphilin controls their mobility and affects short-term facilitation. Cell *132*, 137–148.

Karunanithi, S., Marin, L., Wong, K., and Atwood, H.L. (2002). Quantal size and variation determined by vesicle size in normal and mutant Drosophila glutamatergic synapses. J. Neurosci. *22*, 10267–10276.

Liu, G., Choi, S., and Tsien, R.W. (1999). Variability of neurotransmitter concentration and nonsaturation of postsynaptic AMPA receptors at synapses in hippocampal cultures and slices. Neuron *22*, 395–409.

Marder, E., and Goaillard, J.-M. (2006). Variability, compensation and homeostasis in neuron and network function. Nat. Rev. Neurosci. *7*, 563–574.

Murthy, V.N., Sejnowski, T.J., and Stevens, C.F. (1997). Heterogeneous release properties of visualized individual hippocampal synapses. Neuron *18*, 599–612.

Ribrault, C., Sekimoto, K., and Triller, A. (2011). From the stochasticity of molecular processes to the variability of synaptic transmission. Nat. Rev. Neurosci. *12*, 375–387.

Sankaranarayanan, S., and Ryan, T.A. (2000). Real-time measurements of vesicle-SNARE recycling in synapses of the central nervous system. Nat. Cell Biol. *2*, 197–204.

Sheng, Z.H., and Cai, Q. (2012). Mitochondrial transport in neurons: impact on synaptic homeostasis and neurodegeneration. Nat. Rev. Neurosci. *13*, 77–93.

Stein, R.B., Gossen, E.R., and Jones, K.E. (2005). Neuronal variability: noise or part of the signal? Nat. Rev. Neurosci. *6*, 389–397.

Sun, T., Wu, X.S., Xu, J., McNeil, B.D., Pang, Z.P., Yang, W., Bai, L., Qadri, S., Molkentin, J.D., Yue, D.T., and Wu, L.G. (2010). The role of calcium/calmodulin-activated calcineurin in rapid and slow endocytosis at central synapses. J. Neurosci. *30*, 11838–11847.

Tang, Y., and Zucker, R.S. (1997). Mitochondrial involvement in post-tetanic potentiation of synaptic transmission. Neuron *18*, 483–491.

Verstreken, P., Ly, C.V., Venken, K.J., Koh, T.W., Zhou, Y., and Bellen, H.J. (2005). Synaptic mitochondria are critical for mobilization of reserve pool vesicles at Drosophila neuromuscular junctions. Neuron *47*, 365–378.

Young, S.M., Jr., and Neher, E. (2009). Synaptotagmin has an essential function in synaptic vesicle positioning for synchronous release in addition to its role as a calcium sensor. Neuron *63*, 482–496.

Zador, A. (1998). Impact of synaptic unreliability on the information transmitted by spiking neurons. J. Neurophysiol. *79*, 1219–1229.